Chemical Engineering Journal 171 (2011) 357–367

Contents lists available at ScienceDirect

Chemical Engineering Journal

journal homepage: www.elsevier.com/locate/cej

Preparation, curing kinetics, and properties of a novel low-volatile starlike aliphatic-polyamine curing agent for epoxy resins

Jintao Wan[a,b], Zhi-Yang Bu[a], Cun-Jin Xu[a,c], Bo-Geng Li[a,*], Hong Fan[a,**]

[a] State Key Laboratory of Chemical Engineering, Department of Chemical and Biochemical Engineering, Zhejiang University, Hangzhou 310027, China
[b] Zhejiang Jiamin Plastics Co. Ltd., Jiaxing 314027, China
[c] College of Material, Chemistry and Chemical Engineering, Hangzhou Normal University, Hangzhou 310036, China

ARTICLE INFO

Article history:
Received 12 January 2011
Received in revised form 31 March 2011
Accepted 3 April 2011

Keywords:
Epoxy resin
Curing agent
Polyamine
Isothermal reaction
Model-fitting kinetics
Model-free isoconversional kinetics
Kamal model
Diffusion control
Advanced isoconversional method
Differential scanning calorimetry
Dynamic mechanical analysis
Thermogravimetric analysis

ABSTRACT

A novel low-volatile starlike aliphatic polyamine with extraordinarily high $-NH_2$ functionalities, N,N,N′,N′,N″-penta(3-aminopropyl)-diethylenetriamine (PADT), is synthesized and its molecular structure is confirmed by the FTIR, ^{1}H NMR and ESI-MS analysis. Then PADT is employed as the curing agent for the epoxy resin of diglycidyl ether of bisphenol A (DGEBA) and the isothermal reaction of DGEBA/PADT is systematically investigated with differential scanning calorimetry (DSC) according to the model-fitting approach and model-free advanced isoconversional method developed by Vyazovkin. The result shows that PADT possesses the high reactivity and the reaction is autocatalytic in nature. The further reaction kinetic analysis indicates that the Kamal model can well fit the reaction rate at the reaction-controlled stage, whereas the extended Kamal model with a diffusion term can provide an excellent match throughout the isothermal reaction. On the other hand, the model-free kinetic analysis reveals a strong dependence of effective activation energy, E_α, on fractional conversion, α, which could mirror the drastic change of the reaction mechanisms, in particular, the rapid drop in E_α observed in the deep-conversion regime due to the diffusion-controlled reaction kinetics. Then, a dynamic mechanical analysis (DMA) of the cured DGEBA/PADT network discloses three relaxations from the low- to high-temperature range: β ($T_\beta = -34.4\,^\circ$C), α' ($T_{\alpha'} = 68.0\,^\circ$C) and α ($T_g = 144.3\,^\circ$C). Moreover, compared to linear propanediamine, PADT can much increase the crosslink density and glass temperature of the cured epoxy resin. Finally, the thermogravimetric (TG) analysis reveals PADT, like propanediamine, can impart the cured epoxy resin with the excellent thermal stability with the initial decomposition temperature as high as $\sim$300 °C. On the basis of these experimental data, we can conclude that PADT exhibits a great potential to partially replace conventional high-volatile aliphatic-amine curing agents of low molecular weights.

1. Introduction

Epoxy resins find a broad spectrum of applications in coatings, adhesives, castings, modeling compounds, impregnation materials, high-performance composites, insulating materials, encapsulating and packaging materials for electronic devices, and so forth [1–5]. Due to their great industrial significance, epoxy resins have long been receiving a lot of scientific and technical interests, especially their curing reactions and structure–property relationships. To achieve well-balanced ultimate properties, uncured epoxy resins must be converted into a crosslinked macromolecule in the presence of different kinds of curing agents under optimal curing and processing conditions. Among frequently used curing agents for epoxy resins, amine-based ones, especially aromatic and aliphatic amines, are of prime significance in practical applications. Nowadays, most related scientific work is focused on aromatic-amine curing agents, yet little attention is paid to developing aliphatic-amine ones. Although aromatic-amine curing agents can endow their cured epoxy resins with improved thermomechanical properties and fire resistance, they still suffer from their low reactivity and high melting temperatures. For this reason, high-temperature cure must be applied to improve the compatibility of aromatic-amine curing agents with epoxy resins and to accelerate curing reactions. On the other hand, aliphatic-amine curing agents can well cure epoxy resins at room and even somewhat lower temperatures without heating because they have high reactivity and low melting temperatures, accounting for their principal applications in room-temperature-cure epoxy coatings and adhesives [2].

Traditionally, aliphatic-amine curing agents of low molecular weights have the disadvantages of the strong volatilization, high toxicity, skin irritation and sensitization, fast absorption of carbon dioxide and vapor in air, and strict stoichiometry with respect to epoxy resins [6]. As a result, sometimes they are chemically

* Corresponding author. Tel.: +86 571 87952623; fax: +86 571 87951612.
** Corresponding author. Tel.: +86 571 87957371; fax: +86 571 87951612.
E-mail addresses: bgli@zju.edu.cn (B.-G. Li), hfan@zju.edu.cn (H. Fan).

1385-8947/$ – see front matter © 2011 Elsevier B.V. All rights reserved.
doi:10.1016/j.cej.2011.04.004

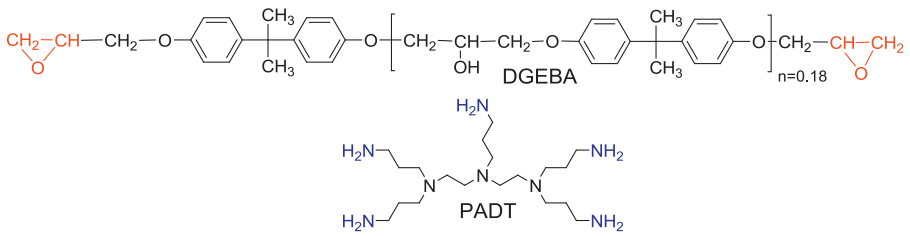

Scheme 1. Molecular structures of epoxy resin (DGEBA) and curing agent (PADT).

modified to form corresponding amine adducts of increased molecular weights to reduce the unfavorable odor, enhance handling safety, extend stoichiometry, decrease toxicity and improve surface appearance of epoxy resins [2,7]. Unfortunately, such modification will sacrifice some desired properties of epoxy resins such as crosslink density, thermal stability and resistance, processability, reactivity, and mechanical strengths. To this end, recently amine acids (i.e., DL-lysine [8] and L-tryptophan [7]) have been used to cure epoxy resins, which take the advantages of the reduced toxicity and environmental friendliness. These curing agents, however, have the high melting points (i.e., 170 °C (decompose) for DL-lysine and (280–285 °C (decompose) for L-tryptophan found at www.sigmaaldrich.com), which leads to their poor compatibility with and low reactivity towards epoxy resins at room temperature, therefore greatly limiting their potential applications in epoxy formulations, especially, room-temperature-cure epoxy coatings and adhesives.

To meet this challenge, the crux of the problem is to develop new aliphatic-amine curing agents with high reactivity and good compatibility, which needs judicious design of their molecular compositions and topology. Exploring aliphatic-polyamine curing agents with nonlinear architectures [9–13] shows a great promise, since lowered bulk viscosity, decreased tendency to crystallize, and reduced toxicity and irritation can be achieved without much sacrificing other desired good properties, in particular, the high reactivity, good compatibility, and crosslink density of cured epoxy resins.

The major objective of this work is to develop and systematically study a novel nonlinear starlike aliphatic-polyamine curing agent for epoxy resins, N,N,N′,N′,N″-penta(3-aminopropyl)-diethylenetriamine (PADT), which quite differs in the molecular topology from common linear aliphatic-amine curing agents. This paper will focus upon the synthesis and characterization of PADT, isothermal reaction, dynamic mechanical properties, and thermal stability of its cured DGEBA system. PADT has high functionalities, low bulk viscosity and very low vapor pressure at room temperature. We shall demonstrate that PADT is highly reactive and can impart its cured epoxy resin with the particularly good thermal properties and significantly increased crosslink density compared to a typical linear aliphatic-amine curing agent (e.g., propanediamine). Especially, this study will afford a deep insight into the isothermal reaction kinetics of DGEBA/PADT by applying the contemporary model-fitting and model-free isoconversional methodologies.

2. Experimental

2.1. Materials

Regent-grade diethylenetriamine and acrylonitrile (Shanghai Reagent Co., Ltd., China) were purified by reduced-pressure distillation prior to use, and propanediamine (99%, Acros Organics) was used as received. DGEBA, diglycidyl ether of bisphenol A, was obtained from Heli Resin Co., Ltd., China with the epoxide equivalent weight (EEW) of 196 g/equiv. Raney nickel, the catalysis for hydrogenation, was prepared by dissolving Al in an Al–Ni alloy (w/w = 50/50, Shanghai Reagent Co., Ltd., China) in NaOH–water solution. PADT, see Scheme 1, N,N,N′,N′,N″-penta(3-aminopropyl)-diethylenetriamine, was prepared in our lab, as detailed in Section 2.2. Other chemicals were used directly without purification.

2.2. Synthesis and characterization of PADT

PADT was prepared with reference to the procedures for preparation of poly(propyleneimine) dendrimers [14,15] with a certain modification. As demonstrated in Scheme 2, the synthesis of PADT begins with bimolecular Michael addition [16] between diethylenetriamine and excessive acrylonitrile under ambient conditions to yield a polynitrile intermediate (PNDT), followed by the heterogeneously catalyzed hydrogenation of PNDT to the corresponding polyamine (PADT), as detailed below.

Magnetically stirred diethylenetriamine (60 g) was diluted slowly at room temperature with distilled water (120 g) in a round-bottom flask (500 ml) fitted with a dropping funnel, stirrer and condensation column, and then excessive acrylonitrile (200 g) was added dropwise with continuous stir in 3 h. After that, the reaction mixture was warmed to 40 °C for 1 h and then heated to reflux (about 80 °C) for additional 20 h. Finally, the unreacted acrylonitrile and water were removed with a rotatory evaporator under reduced pressure, and the obtained crude product was recrystallized from ethanol (3× 800 ml) to afford the nitrile-terminated intermediate, viz. N,N,N′,N′,N″-penta(3-nitrilepropyl)-diethylenetriamine (PNDT), in a good yield (∼94%).

Into a high-pressure autoclave (2000 ml), finely powdered PNDT (100 g), ethanol (95%, 1200 ml), Raney nickel (100 g) and solid NaOH (48 g) were charged. After replacing the air by N_2 three times and then by H_2 three times, the H_2 pressure in the autoclave was increased to 20 atm with continuous agitation (800 rpm). As the reaction progressed, the pressure would decrease gradually. Once the pressure fell down to ≤8 atm, recharge it to 20 atm occasionally. The completion of the whole hydrogenation process would spend about 10–12 h, as indicated by no further decrease in the pressure. Subsequently, release the residual pressure, unload the crude product, filter off the unsolvable solid, and concentrate the filtrate, leading to a two-layer liquid product. The upper organic layer was collected and extracted by toluene combined with a small amount of distilled water three times, then concentrated, and further purified using a silica-gel chromatographic column with menthol as the eluent. Removal of the solvent in the collected fraction afforded the targeting liquid compound (PADT) in slightly yellow (∼76% yield).

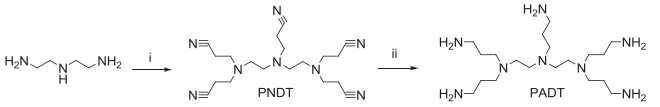

Scheme 2. Synthetic route to N,N,N′,N′,N″-penta(3-aminopropyl)-diethylenetriamine (PADT). i. excessive acrylonitrile, in water, 80 °C for 20 h; ii. Raney nickel, H_2 at 8–20 atm, in ethanol–water (95/5, v/v), room temperature for 10–12 h.

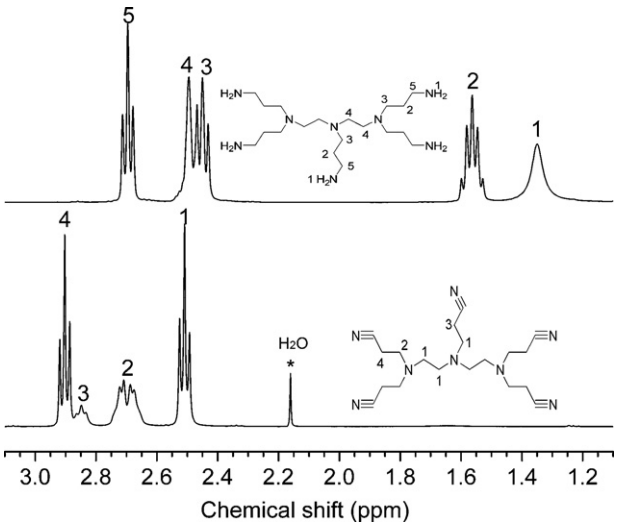

Fig. 1. ^{1}H NMR spectra of nitrile-terminated intermediate (PNDT) and targeting product (PADT).

^{1}H NMR spectra of PADT and PANT, and ESI-MS spectrum of PADT are presented in Figs. 1 and 2 from which we can confirm that the spectral data of PADT are in line with the estimated from its molecular structure, indicating the full achievement of PADT.

PADT: FTIR (υ_{max}, cm^{-1}) 3353 (NH_2, υ_{as}), 3285 (NH_2, υ_s), 2937 (CH_2, υ_{as}), 2860 (CH_2, υ_s), 1593 (NH_2, δ), 1466 (CH_2, δ). ^{1}H NMR (400 MHz, in $CDCl_3$) δ ppm 2.51, t, 10H, N–C*H*$_2$–C*H*$_2$–N(C*H*$_2$–)–C*H*$_2$–C*H*$_2$–N; 2.63–2.76, m, 8H, N–C*H*$_2$CH$_2$CN; 2.85, t, N–CH$_2$C*H*$_2$CN, 2H; 2.90, t, 8H, N–CH$_2$C*H*$_2$CN. ESI-MS: $[M+1]^+$ = 389.2 (calculated 389.4).

2.3. DSC measurement

The isothermal reactions of DGEBA/PADT were monitored with a differential scanning calorimeter (DSC, Perkin Elmer 7) calibrated with an indium standard (99.999%) before any measurements. The isothermal reaction was monitored for the different temperatures of 40, 50, 60 and 70 °C, after which a second run was followed with the heating rate of 10 °C/min from 25 to 250 °C to determine the residual reaction heat. Stoichiometric DGEBA and PADT were mixed homogeneously as quickly as possible under vigorous stirring at room temperature (<15 °C), and each prepared mixture was used only once. The fresh reaction mixture (about 10 mg) was sealed in an aluminum DSC pan and immediately heated to the preset reaction temperature at 100 °C/min to carry out an isothermal scan with an identical empty pan as the reference. In addition, the glass temperature of the completely cured epoxy resin was determined as the middle fluctuation point of the specific heat from an additional heating run with the temperature ramp of 10 °C/min from 25 to 250 °C. Furthermore details about how to conduct isothermal DSC experiments and how to process isothermal calorimetric data could be accessed elsewhere [17].

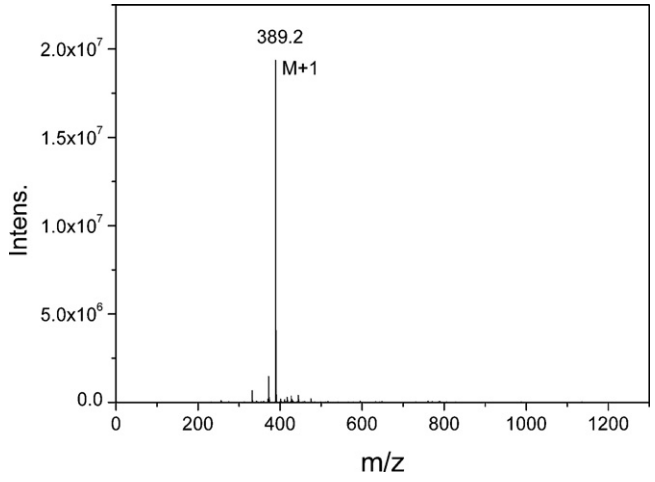

Fig. 2. ESI-MS spectrum of PADT.

2.4. DMA test

Stoichiometric DGEBA and PADT were mixed well with stirring at room temperature, and then the mixture was poured into a preheated stainless-steel mould (40 °C) coated with a thin layer of a silicone releasing agent. The filled mould was placed in vacuum to drive off any bubbles, and then transferred into an air-blast oven according to the curing schedules: 70 °C for 1.5 h and 150 °C for another 2.5 h. After cooling the mould to room temperature and demoulding, the cured casting epoxy bars were obtained which were machined to the rectangle specimens with the dimension of 35 mm × 10 mm × 2 mm. The specimens were subjected to a thermomechanical test using a dynamic mechanical analyzer (DMA Q800, TA Instruments), and the specific operation parameters were given below. The heating rate was 3 °C/min, the loading frequency was 1 Hz, the oscillation amplitude was 15 μm, the temperature ranged from −100 °C to well the above glass temperature of the completely cured epoxy resin, and the clamp is a single cantilever one. In addition, for the comparative study, the cured DGEBA/propanediamine specimens were prepared and tested with DMA according to the same procedure as used for preparation of the DGEBA/PADT ones.

2.5. TG measurement

Thermal stability of cured DGEBA/PADT and DGEBA/propanediamine were evaluated using a thermogravimetric analyzer (Pyris 1 TGA) operated at a constant heating rate of 10 °C/min from 40 to 850 °C under dynamic N_2 protection (40 ml/min). About 2 mg of the cured epoxy resin was loaded in a white mica crucible without a lid.

3. Results and discussion

3.1. Theoretical aspects

Thermosetting resins find very important industrial applications due largely to their wide formulations and property diversity compared to conventional thermoplastic resins. To achieve optimal end-use properties and to stabilize the quality of derivative thermosetting materials, one must carefully control the curing conditions which will greatly affect their shaping processes, morphology evolution, ultimate microstructures, and internal stress developed during cure [18–23]. Thus, it is imperative to accumulate adequate kinetic knowledge about thermosetting reactions from scientific and practical application perspectives. Although the reaction kinetics of thermosetting resins can be studied by many different analytical methods, in most cases DSC is particularly welcome due to easy in sample preparation and great in accuracy, in particular, for kinetic investigations of highly exothermic epoxy reactions [17,24]. Providing that curing reactions of epoxy resins are only a thermal event, measured DSC heat flow is assumed to be directly proportional to reaction rate of epoxy groups; thus, fractional conversion of epoxy groups, briefly conversion henceforth,

can be written by Eq. (1):

$$\alpha = \frac{\int_0^t H dt}{\int_0^{t_f} H dt} \tag{1}$$

where α is the conversion or the extent of cure, H is the DSC heat flow, t is the reaction time, and t_f is the time to full conversion.

Nowadays, model-fitting and model-free isoconversional methodologies [25–29] are most often applied to curing reaction kinetic studies of epoxy resins, which are sometime used complementarily. For the former, a reaction model should be assigned previously with which to fit experimental data (reaction or conversion) for estimating model-related kinetic parameters. Specifically, the kinetic models most frequently utilized to describe isothermal reactions of epoxy resins fall into simple nth-order reaction model (Eq. (2)) [30] and autocatalytic Kamal model (Eq. (3)) [31–33].

$$\frac{d\alpha}{dt} = k(T)(1-\alpha)^n \tag{2}$$

$$\frac{d\alpha}{dt} = [k_1(T) + k_2(T)\alpha^m](1-\alpha)^n \tag{3}$$

In these equations, $k(T)$ is the temperature-dependent reaction rate constant, $k_1(T)$ is the non-autocatalytic rate constant, $k_2(T)$ is the autocatalytic rate constant, and m and n are the reaction orders corresponding to $k_1(T)$ and $k_2(T)$. All these rate constants meet the classic Arrhenius equation:

$$k = A\ \exp\left(\frac{-E_a}{RT}\right) \tag{4}$$

where A is the pre-exponential factor and E_a is the activation energy.

On the other hand, the model-free kinetic methodology with the advantage of not assuming any specific reaction model, just holds the assumption that the reaction rate is merely a function of temperature T, as expressed by Eq. (5) [34,35]:

$$\left[\frac{d\ \ln(d\alpha/dt)}{dT^{-1}}\right]_\alpha = -\frac{E_\alpha}{R} \tag{5}$$

where E_α is the effective energy [36] for a specific conversion, α. By Eq. (5), several isoconversional methods with different analytic expressions have been developed with which one can obtain a correlation of E_α with α for a thermal process of interest. Among them, the most frequently cited in literature is the well-known linear Flynn–Wall–Ozawa method, briefly FWO method [37,38]; however, it is only applicable to nonisothermal processes with multiple linear temperature programs. Alternatively, the advanced isoconversional method developed by Vyazovkin [39–41] (i.e., the Vyazovkin method), is capable of processing both isothermal and nonisothermal data with the exactly same computational method combined with unparallel precision attainable, because of the more advanced nonlinear algorithm adopted in this method.

According to the Vyazovkin method, a series of thermal experiments need to be conducted in terms of different temperature programs, and then E_α can be determined for any specific α by minimizing Eq. (6):

$$\Phi(E_\alpha) = \sum_{i=1}^{n}\sum_{j\neq i}^{n}\frac{J[E_\alpha, T_i(t_\alpha)]}{J[E_\alpha, T_j(t_\alpha)]} = \min \tag{6}$$

$$J[E_\alpha, T_i(t_\alpha)] \equiv \int_{t_{\alpha-\Delta\alpha}}^{t_\alpha} \exp\left[\frac{-E_\alpha}{RT_i(t)}\right] dt \tag{7}$$

In Eqs. (6) and (7), subscripts, i and j, denote the different thermal experiments conducted with varied temperature programs, $\Delta\alpha$ is the small increment in α (usually $\alpha \approx 0.02$, which is enough to effectively eliminate accumulative errors during calculating E_α), and the integral J can be well approached numerically with a trapezoid rule. Repeat this minimization procedure for each α of interest and an E_α–α correction will result. The more detailed descriptions of how to use the Vyazovkin method to process isothermal calorimetric data can be accessed elsewhere [39,42]. After knowing E_α–α relationship, one can perform the kinetic predication for a thermal process of interest by using Eq. (8) [27,43]:

$$t_\alpha = \frac{J[E_\alpha, T_i(t_\alpha)]}{\exp[-E_\alpha/RT_0]} \tag{8}$$

where t_α is the reaction time to any specific conversion, α, T_0 is the arbitrary isothermal temperature of interest, and other parameters have the same meaning as in Eqs. (5)–(7). In principle, with Eq. (8) one can predict the reaction time for a thermosetting curing reaction to progress to any specific conversion, α.

To date, the Vyazovkin method has been successfully applied to epoxy resins [34,42,44–49], melamine–formaldehyde resins [50], phenolic resins [51,52], furan resins [53], etc., for probing the isothermal reaction mechanisms as well as conducting the isothermal reaction kinetic predications. In this context, the Vyazovkin method has been used to inspect the kinetic mechanisms of the isothermal DGEBA/PADT reaction, and the involved kinetic prediction will be discussed in our proceeding paper in combination with the nonisothermal DSC data which can cover the whole conversion range.

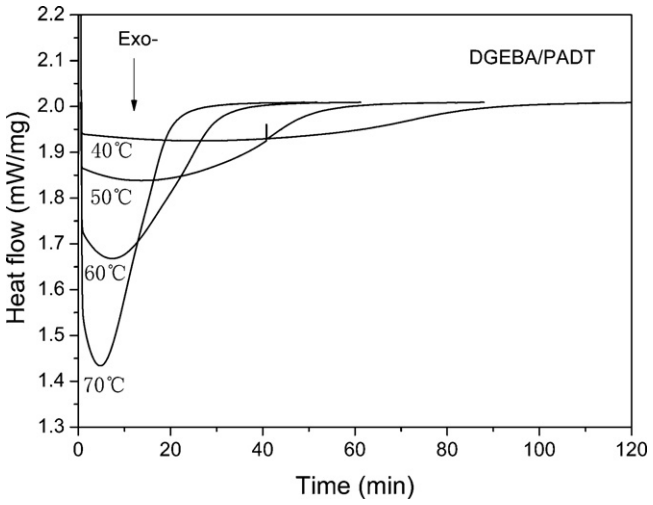

Fig. 3. Isothermal thermographs of heat flow against reaction time for 40, 50, 60 and 70 °C.

3.2. Curing reaction and kinetic modeling

Fig. 3 presents the DSC heat flow as a function of time of DGEBA/PADT with the different reaction temperatures of 40, 50, 60 and 70 °C. All the DSC traces show only a single exothermic peak, which indicates that the only reaction involved is the amine-epoxy addition without interference of side reactions. Note here that because the isothermal reaction temperatures applied are relatively low (≤70 °C) and the epoxy groups and the amino hydrogens are in a stoichiometric balance, thus the etherization reaction between the epoxy and hydroxyl groups can be safely neglected [54,55]. Integrating the peak with respect to the horizontal baseline for the different temperatures results in the corresponding isothermal reaction enthalpy; the isothermal reaction enthalpy plus the residual reaction enthalpy produces the overall reaction enthalpy. The obtained isothermal reaction exotherm for 40, 50, 60 and 70 °C is 80.1, 93.6, 100.4 and 104.3 kJ/mol epoxide, respectively, and the

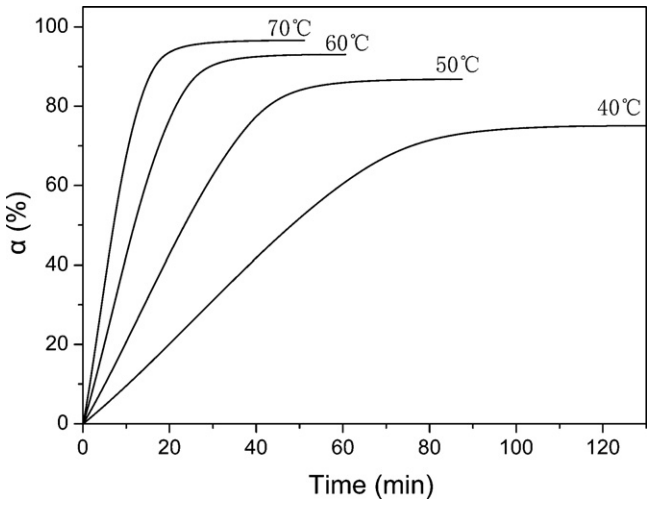

Fig. 4. Fractional conversion α as a function of time t for 40, 50, 60 and 70 °C.

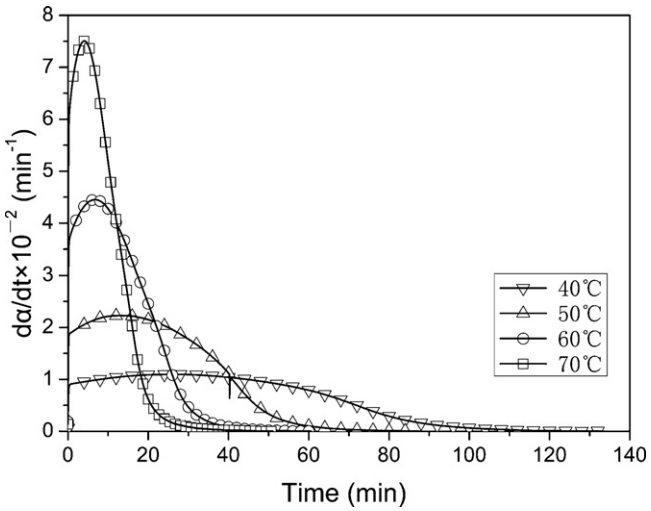

Fig. 6. $d\alpha/dt$ as a function of t for 40, 50, 60 and 70 °C.

total reaction exotherm is 107.9 kJ/mol epoxide, which agrees with the typical value (98–122 kJ/mol epoxide) for conventional epoxy-amine polymerizations [9,10,56]. This agreement implies that the N–H functionalities of PADT have high reactivity and PADT can well cure the epoxy resin to a fully acceptable reaction extent from a practical application consideration.

With Eq. (1) the isothermal data presented in Fig. 2 can be transformed into the conversion α as a function of time t. Fig. 4 gives the obtained α–T curves, where α increases rapidly with increasing t at the early stage of the reaction, then the increase slows down, and eventually α levels off to a limiting conversion, α_T. α_T increases with the reaction temperatures, while t decreases systematically; for instance, a rise in the temperature from 40 to 70 °C leads to an increase in α_T value from 0.751 to 0.966. Despite that, under such isothermal conditions, only a limited α_T value ($\alpha_T < 1$) can be reached, indicating the incomplete cure, as a result of the diffusion limitation at the deep-conversion stage. The diffusion-controlled reaction kinetics can be attributed to the vitrification of the reaction system, because the isothermal temperatures are much lower than the glass temperature of the completely cured epoxy resin ($T_{g\infty}$ = 121 °C, see Fig. 5). To illustrate, as the isothermal reaction progresses, the glass temperature of the reaction system will increase steadily with conversion and even exceed the isothermal reaction temperature, thereby leading to the vitrification. In this case, the thermal motions of the network chains having reactive groups become significantly restricted, which will eventually cause the temporary stop of the reaction in the deep glassy state unless the reaction temperature is elevated higher to devitrify the reaction system [6,57–61]. More fundamentally, as the curing reaction proceeds in the glassy state, slower and slower becomes the diffusion rate of the reactive species to a tangible distance to ensure the taking place of the further reaction, even beyond the experimental observation limit. As the reaction progressed into the deep-glass state, there is no sufficient "free volume" to accommodate the configuration adjustment of the molecular segments, in which case a number of the reactive groups are "frozen" in the network, ultimately leading to the incomplete cure.

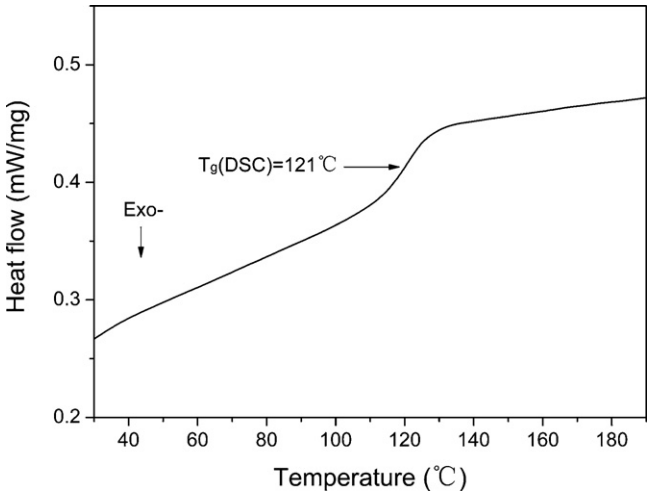

Fig. 5. DSC curve of fully cured DGEBA/PADT with heating rate of 10 °C/min.

Differentiating the conversional curves (Fig. 5) with respect to t gives rise to the reaction rate $d\alpha/dt$. As shown in Fig. 6, $d\alpha/dt$ increases almost linearly with t initially, arriving at its maximum at the moment $t > 0$ instead of at the onset of the reaction ($t \to 0$), and increasing the temperature leads to the increased maximum $d\alpha/dt$ and reduced reaction time. The time to maximum $d\alpha/dt$ not zero indicates that the isothermal reaction of DGEBA/PADT is autocatalytic in nature [62,63], so that it is more appropriate to adopt the autocatalytic Kamal model, Eq. (3), to fit the reaction rate, thus excluding the simple nth-order model, Eq. (2). While the reaction is progressing in the deep-conversion stage, $d\alpha/dt$ falls down rapidly approaching zero, which indicates that the reaction is significantly inhibited in the highly crosslinked network.

After a certain transformation of the experimental data, the dependence of $d\alpha/dt$ on α can be obtained; see the solid lines in Fig. 7. This figure clearly illustrates that all the $d\alpha/dt$–α curves reach its peak value at the approximately unchanged conversion of about 0.3 irrespective of the reaction temperatures, which is indicative of the autocatalytic reaction, in agreement with the main conclusion extracted from Fig. 6. Also, the isoconversional peak reaction rate implicates that the autocatalytic characteristic observed is due primarily to the chemical factors, i.e., the –OH groups generated during the epoxy-amine reaction, which can considerably catalyze the further epoxy-amine reactions [64].

Return to the Kamal model, Eq. (3), in which k_1 can be estimated by extrapolating the $d\alpha/dt$–α curve (Fig. 7) to $\alpha = 0$. Then, after introducing the obtained k_1 value into Eq. (3), the other three parameters, k_2, m and n, can be determined by fitting the experimental data with a least-squared procedure of the OriginPro 7.5 (OriginLab Co.), and their obtained values are summarized in Table 1. As can be seen, as the temperature rises, k_1 and k_2 increase

Table 1
Isothermal limiting conversion α_T and calculated kinetic parameters for Kamal model, Eq. (3).

T_c (°C)	40	Error	50	Error	60	Error	70	Error
α_T	0.751	–	0.868	–	0.930	–	0.966	–
k_1 (min^{-1})	0.00903	7.7×10^{-7}	0.018619	1.9×10^{-6}	0.0364049	6.7×10^{-6}	0.058703	3.5×10^{-5}
k_2 (min^{-1})	0.02564	3.0×10^{-5}	0.03867	6.0×10^{-5}	0.08164	1.0×10^{-4}	0.13187	1.5×10^{-4}
m	0.99976	3.7×10^{-4}	0.94473	6.7×10^{-4}	0.93345	6.2×10^{-4}	0.85832	3.7×10^{-4}
n	1.18822	6.6×10^{-4}	0.91811	7.1×10^{-4}	0.97166	5.3×10^{-4}	0.96225	4.7×10^{-4}
$m+n$	2.18798	1.0×10^{-3}	1.86284	1.4×10^{-3}	1.90511	1.2×10^{-3}	1.82057	8.4×10^{-4}
R^2	0.99903	–	0.99848	–	0.99972	–	0.99966	–

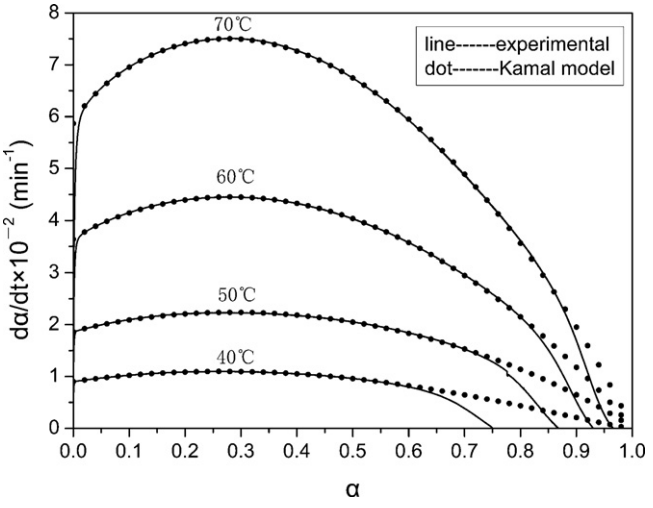

Fig. 7. Comparison of experimental $d\alpha/dt$ with that predicated from Eq. (3).

systematically, whereas m, n and their sum, $m+n$, depend moderately on the temperature, which could, to some extent, mirror the complexity involved in the curing reaction [48,65,66].

Fig. 8 presents the linear plots of $\ln k_1$ and $\ln k_2$ against $1/T$ in the light of the Arrhenius equation, Eq. (4), from which a good linear correlation can be established ($R_1{}^2 = 0.9979$ and $R_2{}^2 = 0.9857$). The slopes of the fitted lines give rise to the activation energies for the non-autocatalytic and autocatalytic reactions, E_{a1} and E_{a2}. E_{a1} (56.28 ± 2.56 kJ/mol) is somewhat higher than E_{a2} (50.50 ± 4.30 kJ/mol), which can validate that the autocatalytic reaction needs to overcome a lower energetic barrier than the non-autocatalytic reaction. The autocatalytic reaction can be attributed to the accumulation of the –OH groups in the reaction system as the reaction goes on, which results in the increased percentage of the epoxy-amine reaction taking place via the hydroxyl-assisted autocatalytic mechanism [56,64,67].

Experimental $d\alpha/dt$ and the predicated from the Kamal model, Eq. (3), are compared in Fig. 9, where the points represent the estimated rate and the lines the experimental. This figure clearly shows that experimental $d\alpha/dt$ agrees well with the predicated up to a critical conversion which increases with the temperature, after which the noticeable derivation can be observed due to the diffusion-controlled reaction kinetics [68]. In other words, the Kamal model can satisfactorily describe the reaction rate in the reaction-controlled stage, yet still functions less well in the diffusion-controlled domain.

To completely describe the diffusion-controlled epoxy cure, Cole [69] has extended the Kamal model by coupling a diffusion factor $f(\alpha)$, arriving at

$$\frac{d\alpha}{dt} = [k_1(T) + k_2(T)\alpha^m](1-\alpha)^n f(\alpha) \tag{9}$$

In Eq. (9), $f(\alpha)$ is defined as

$$f(\alpha) = \frac{k_e}{k_c} = \frac{1}{1+\exp[C(\alpha-\alpha_c)]} \tag{10}$$

where k_e is the effective rate constant, k_c is the chemical reaction rate constant predicated from Eq. (3), C is the fitting constant, and α_c is the critical conversion, which indicates an abrupt transition from reaction to diffusion control. In what follows, the extended Kamal model will be utilized to describe the isothermal DGEBA/PADT reaction rate over the entire conversion range of interest.

Dividing the experimental rate by that predicated from the Kamal model produces the curve of $f(\alpha)$ vs. α. As seen in Fig. 8, $f(\alpha)$ approximately equals unity up to a critical conversion, but after that sharply falls down to zero in a narrow conversion interval. The decrease of $f(\alpha)$ will be observed at a higher-conversion regime if the reaction temperature is increased. This finding suggests that

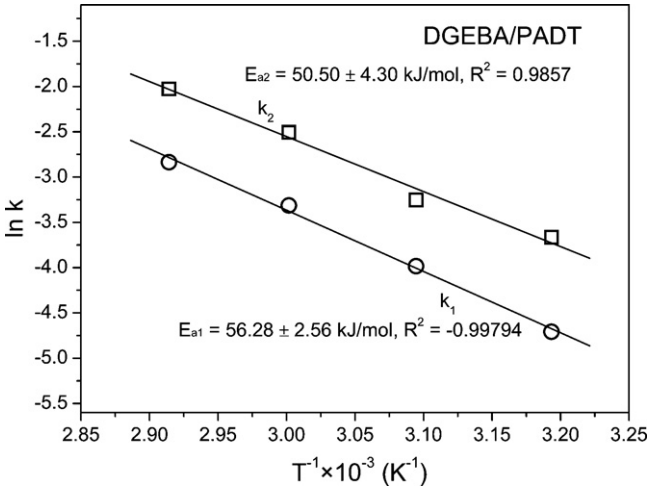

Fig. 8. Arrhenius plots of $\ln k_1$ and $\ln k_2$ vs. $1/T$ for calculating E_{a1} and E_{a2}.

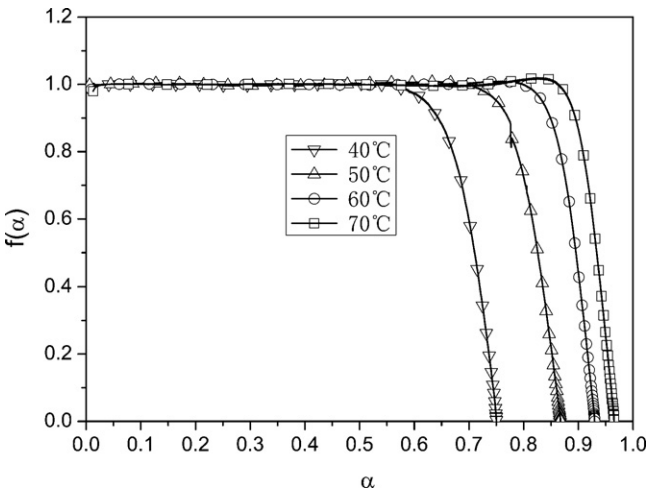

Fig. 9. Diffusion factor $f(\alpha)$ as a function of conversion α for 40, 50, 60 and 70 °C.

Table 2
Values of critical conversion α_c and fitting constant C for Eq. (10).

T_c (°C)	40	50	60	70
α_c	0.7057	0.82198	0.8927	0.93148
C	52.61183	54.99021	67.0288	72.72027

the isothermal reaction has traversed both the reaction-controlled regime and the diffusion-controlled domain, and the higher the temperature, the greater the critical conversion after which the diffusion control occurs. After substitution of the $f(\alpha)$–α data into Eq. (10), α_c and C can be determined by using a least-squared procedure of the Origin 7.5. As can be seen in Table 2, α_c and C increase systematically with T_c, which can quantitatively substantiate that elevating the reaction temperature delays the diffusion-controlled kinetics, leading to its occurrence in the deeper-conversion range, because the mobility of the network chains is enhanced at the higher reaction temperature.

So far, the explicit rate equations can be established by introducing a complete set of the obtained kinetic parameters into the extended Kamal model, Eq. (9), and then they are used to model the reaction rate. The predicted $d\alpha/dt$ and the experimental one are compared in Fig. 10, from which an excellent agreement can be found. Therefore, the extended Kamal model is adequate to simulate the reaction rate throughout the entire isothermal DGEBA/PADT reaction, and the model-fitting kinetic study ends with a satisfactory result.

3.3. Model-free isoconversional kinetics

In reality, curing reactions of thermosetting polymers in condensed matter are rather complex, complicated by a number of elementary reactions, mass-transfer processes and phase changes, which will result in rather complex reaction kinetic mechanisms [70,71]. To gain a deeper insight into the isothermal reaction of DGEBA/PADT, here the advanced isoconversional method (the Vyazovkin method) is utilized to derive the dependence of effective activation energy E_α upon conversion α, on the basis of which the reaction mechanisms are discussed in detail. It has frequently demonstrated that E_α–α correlations can provide instructive information and useful clues about kinetic mechanisms of thermally stimulated processes in polymers [34]. According to this method, introduce the α–t data shown in Fig. 2 into Eqs. (6) and (7), and then by minimizing Eq. (6), E_α at any particular α can be estimated,

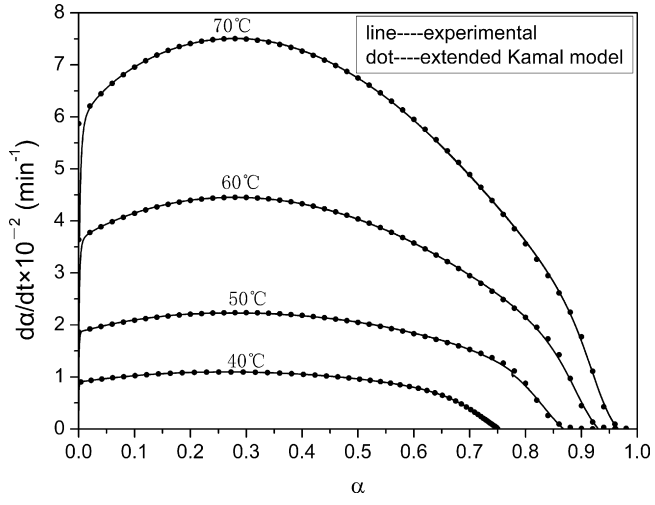

Fig. 10. Comparison of experimental $d\alpha/dt$ with simulation from extended Kamal model, Eq. (9).

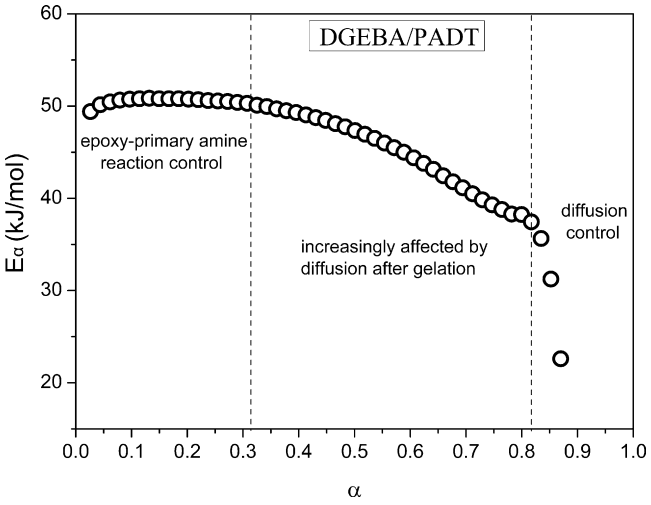

Fig. 11. Effective activation energy E_α as a function of conversion α.

thereby yielding the correlation of E_α with α. As illustrated in Fig. 11, E_α depends greatly on α, which suggests the reaction seems to follow the multi-step reaction mechanisms associated with the different kinetic steps with varying energetic barriers [34,45,46,65]. The detailed discussion on this correlation is as follows.

Fig. 11 shows that at the low-conversion stage, E_α exhibits a relatively constant value of ~50 kJ/mol up to $\alpha \approx 0.32$, which can be ascribed to the reaction between the epoxy groups of DGEBA and the primary amino groups of PADT, since the primary amine is more reactive than the newly formed secondary amine during the reaction due to their increased steric hindrance [12,47,48,72]. Moreover, the theoretical gelation conversion of the stoichiometric DGEBA/PADT system, $\alpha_{gel} \approx 0.333$, can be estimated from Eq. (11) [73]:

$$\alpha_{gel} = \left[\frac{1}{(f_A - 1)(f_E - 1)}\right]^{\frac{1}{2}} = \left[\frac{1}{(10 - 1)(2 - 1)}\right]^{\frac{1}{2}} \approx 0.333 \qquad (11)$$

where f_A is the functionality of the curing agent and f_E is the functionality of the epoxy resin. Note here that estimated α_{gel} is slight higher than the aforementioned break conversion of 0.32 before which E_α remains relatively constant. This finding indicates that in this stage, the curing reaction is still not complicated by the gelation, and thus it is possible for the reactive groups to diffuse a relatively long distance (the long-range motion) to react with each other. For this reason, although the viscosity of the reaction system rapidly increases with increasing conversion, the diffusion is still less influential relative to the chemical reaction in determining the overall reaction rate, accounting for the reaction-controlled reaction kinetics within the low-conversion reaction stage.

As α continues to increase above ~0.32, E_α decreases gradually from ~50 to ~40 kJ/mol up to $\alpha \approx 0.82$, which could be interpreted as follows. After the reaction traversing the early conversion stage, a large number of the –OH groups have been produced in the reaction system which can considerably catalyze the further reaction, for which reason the associated energetic height for the further epoxy-amine reaction is lowered. More importantly, the gelation occurs at the beginning of this stage ($\alpha_{gel} \approx 0.333$), leading to the formation of the crosslinked network. As the reaction further progresses, the gelation fraction increases and the sol fraction decreases in turn, which will lead to the ever tighter network. The diffusion of the reacting species in the crosslinked network becomes increasingly restricted, because the number of the crosslink increases steadily as α continues increasing. From this consideration, the further curing reaction will rely mainly on the short-range motions of the molecular segments to ensure the reactive groups to diffuse into a tangible

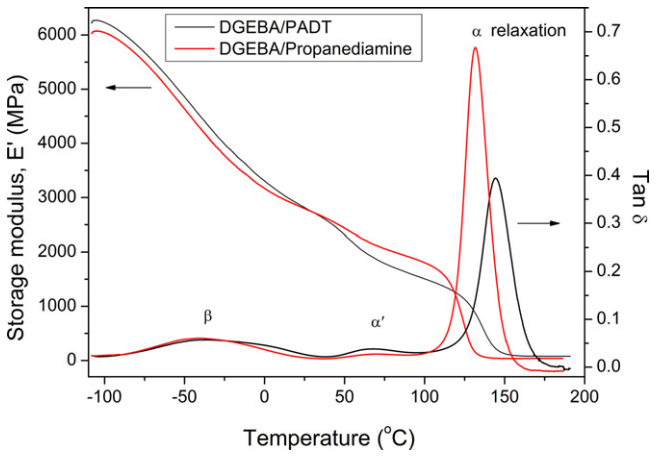

Fig. 12. Dynamic mechanical spectra for storage modulus, E', and damping factor, tan δ, against temperature with heating rate of 3 °C/min for DGEBA/PADT and DGEBA/propanediamine networks.

distance and react with each other, which could lead to the gradual decrease of the energetic barrier associated with the diffusion of the reactive groups.

As α further increases beyond ~0.8, even its slight increment can cause a dramatic reduction in E_α; for example, in this narrow conversion range E_α decreases from ~40 to less than ~20 kJ/mol until the practical stop of the isothermal reaction, which implies that the diffusion control has completely turned over the reaction control, becoming the decisive factor for determining the overall kinetic rate [74]. The diffusion-controlled kinetics can be due to the taking place of the vitrification in the reaction system, after which the motions of the network chains bearing the reactive groups are greatly restricted, resulting in the much increased diffusion time [68]. More specifically, once the reaction system approaches its glassy state and thereafter, the mass transfer of the reactive species will spend much more time than the pure chemical reaction itself, so that the reaction is in the diffusion control [42]. Furthermore, Stutz and co-workers [75,76] have experimentally proved that while curing reactions of thermosets proceeding in the glass-transition region, the reactions exhibited the very low activation energy, because the short-range segmental motions (even the motions in a much smaller scale) became increasingly significant in determining the overall reaction rate.

To conclude, for the isothermal reaction considered here the reaction control holds the leading position at the early stage of the cure, and the diffusion control is much more operative in the deep-conversion stage, as the reaction system approaches its glass-transition regime and thereafter.

3.4. DMA result

Fig. 12 plots the dynamic storage modulus, E', and damping factor, tan δ, as a function of temperature with the constant heating rate of 3 °C/min, while Table 3 lists the characteristic relaxation temperatures and modulus collected from this figure. As can be see from Fig. 12 and Table 3, E' is rather great at the low temperature (e.g., −100 °C), which is meant that the network can only be slightly deformed under a given load. As the temperature rises, there appears a small but broad damping peak for tan δ in −70 to 20 °C, which is associated with the β relaxation of the network stemming from the crankshaft motions of hydroxypropylether sequences (CH_2–CHOH–CH_2–O–) [77–79]. In the higher temperature range (i.e., >100 °C) a major relaxation can be observed, as indicated by the dramatic change in tan δ and E'. To illustrate, E' decreases rapidly in this narrow temperature range, reaching a plateau with the small but relatively constant value of <100 MPa (Table 3), while tan δ goes through its maximum. These dramatic changes are due to the glass–rubber transition of the DGEBA/PADT network, and accordingly the glass-transition temperature (T_g) is 144.3 °C for tan δ_{max}, which is comparable with T_g of most epoxy networks cured with conventional linear aliphatic amines [79–81]. Notice here that the glass temperature (144.3 °C) determined with DMA is somewhat higher than that measured with DSC (121 °C). This difference is originated from the different kinds of the temperature responses of the monitored properties determined with the different analytic methods, and specifically DMA measures the thermomechanical response of the network, whereas the DSC detects the change of specific heat. No doubt, the change of the dynamic mechanical property and specific heat with temperature is not always in-phase, which strongly depends on specific testing conditions. Therefore, it is more reasonable to compare the glass temperature of the different epoxy networks under the exactly same testing condition in terms of the same standard.

Table 3
Characteristic relaxation temperatures and modulus and crosslink density of DGEBA/PADT and DGEBA/propanediamine networks.

Formulation	DGEBA/PADT	DGEBA/propanediamine
α-relaxation (T_g)/°C	144.3	131.8
α'-relaxation ($T_{\alpha'}$)/°C	68.0	–
β-relaxation (T_β)/°C	−34.4	−39.9
Modulus at −100 °C/MPa	6231	6044
Modulus at 20 °C/MPa	2901	2860
Modulus at 80 °C/MPa	1727	2011
Rubber Modulus at T_g + 30 °C/MPa	79	37
Crosslink density (ν_e)/mol m^{-3}	7079	3144

To further elucidate the molecular topology of PADT on the rigidity and relaxations of the corresponding network, E' and tan δ of DGEBA cured with starlike PADT and representative linear propanediamine are compared in Fig. 12 and Table 3. The result shows that DGEBA/PADT has a somewhat higher E' value below the room temperature range than DGEBA/propanediamine, but a reverse outcome appears at the higher temperature range (>30 °C). A quite similar finding has been revealed by Cukierman et al. [78] for other epoxy-amine networks, which can be related to the crosslink density of the epoxy network. Specifically, because PADT contains three tertiary amine groups (N^t) per molecule, predictably, they can function as the extra crosslinks in the resulting epoxy network, thus contributing to the crosslink density positively. In fact, this predication will turn out to be true shortly in this subsection. The increased crosslink density will cause the increased elastic energy dissipated as heat during the relaxation motions of the hydroxypropylether sequences (β relaxation), because the more spatial rearrangements and cooperative motions of the neighboring network chains have to be invoked to accommodate the configuration adjustment of the hydroxypropylether units, thus resulting in the increased damping [78]. In addition, DGEBA/PADT exhibits the higher β relaxation temperature than DGEBA/propanediamine, which can be attributed to the much restricted relaxation motions of the hydroxypropylether segments in the former network also due to the increased crosslink density.

More importantly, the glass temperature of DGEBA/PADT is 12.6 °C higher than that of DGEBA/propanediamine, which indicates that the improved thermal resistance and upper service temperature of the former. Note herein that, for the glass relaxation, DGEBA/PADT manifests the decreased peak height for tan δ_{max} compared to DGEBA/propanediamine, which likely indicates the decreased elastic energy dissipated during the glass–rubber transition. The finding means that PADT makes the resulting network more rigid; thus, the plastic deformation of the network decreases, whereas the elastic deformation increases under a given load. The

reason lies in that the much more tightly crosslinked DGEBA/PADT network makes the cooperative motions of the whole network chains easier during the glass relaxation since the averaged chain length is considerably shortened, which leads to the reduced phase lag between the stress and strain formed in the network under action of an external force. This could account for the decreased damping observed during the glass relaxation of the DGEBA/PADT network.

From the analysis above, the crosslink density of the DGEBA/PADT network shows great interest, which can probably reflect the distinctive characteristic of the network, because PADT has the starlike molecular architecture and extraordinary high functionalities. To be quantitative, we estimate the crosslink density of the DGEBA/PADT network and the DGEBA/propanediamine control by using Eq. (12) [82–87]:

$$E_r = 3RT_r\nu_e \quad (12)$$

where E_r is the rubber modulus which can be regards as $T_g + 30$ [88], R is the universal gas constant, T_r is the temperature corresponding to E_r, and ν_e is the crosslink density. The calculated ν_e with corresponding E_r is listed in Table 3. The result clearly shows that DGEBA/PADT has the much higher ν_e value than DGEBA/propanediamine, which can quantitatively justify our previous postulation that PADT imparts its cured epoxy network with the increased crosslink density. The increased crosslink density lies in that that PADT has three tertiary amine groups (N^t), which can function as the additional crosslinks in the corresponding network. Note here that although PADT has the higher N–H equivalent weight (38.9 g/mol) than propanediamine (18.5 g/mol), accounting for its extended stoichiometry towards DGEBA and thus facilitating weighting and well mixing, the additional crosslinks inherited from the PADT molecules seem much more determinative to the crosslink density, resulting in the increased crosslink density of the DGEBA/PADT network. Also, the increased crosslink density is responsible for the appreciably increased glass temperature of the DGEBA/PADT network compared with the DGEBA/propanediamine control.

In addition to the α and β transitions discussed above, a minor transition (α') can be indentified for the DGEBA/PADT network in 30–100 °C, but this transition cannot be clearly detected in the DGEBA/propanediamine control in the same temperature range, which is unique to PADT. What is the origination of this mirror transition? To answer this question, let us compare the molecular structures of PADT and propanediamine. Clearly, PADT has the starlike branched molecular topology with three tertiary amine groups as the branching points, whereas linear propanediamine has no such branched points. For this reason, we can infer that the three tertiary amine groups inherent from PADT are responsible for the α' relaxation observed in the DGEBA/PADT network. To illustrate this point, since these tertiary amine groups themselves serve as the extra crosslinks in the DGEBA/PADT network, the local cooperative motions of their connected flexible aliphatic molecular chains need to overcome a higher energetic barrier to relax in the confined environment.

In short, on the basis of the analysis above, we can rationally conclude that PADT endows its cured epoxy resin with the fully acceptable upper service temperature, improved glass temperature, enhanced damping in the β relaxation, and, in particular, significantly increased crosslink density.

3.5. TG analysis

Fig. 13 presents the TG thermographs for the weight and derivative-weight percentage (decomposition rate) against temperature for the DGEBA/PADT and DGEBA/propanediamine systems with the heating rate of 10 °C/min in N_2. The result clearly

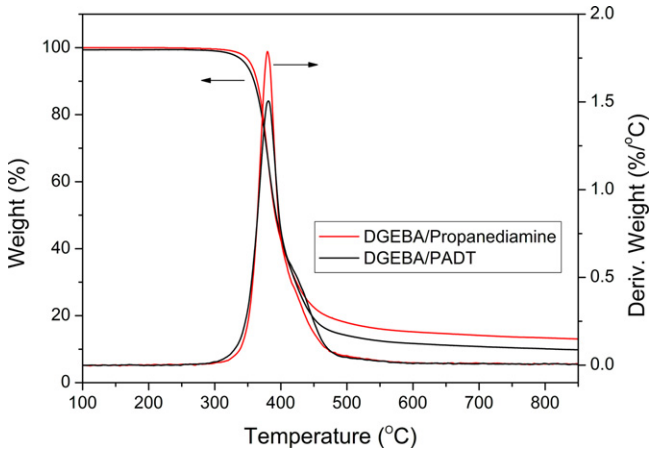

Fig. 13. TG thermographs of cured DGEBA/PADT and DGEBA/propanediamine with heating rate of 10 °C/min in N_2.

shows that no obvious weight loss can be found up to ~300 °C, which suggests that both linear propanediamine and PADT can impart their cured epoxy resin with sufficient good thermal stability. Besides, the initial thermal decomposition temperature of the epoxy resins has no much difference, which indicates that PADT, comparable to propanediamine, which can serve as a representative curing agent in linear aliphatic-amine series, can endow the cured epoxy resin with the sufficient good thermal stability. This finding also suggests that the onset of the thermal degradation of the amine-cured epoxy resin is primarily determined by the basic element composition of networks, instead of by the crosslink density. By comparatively examining glass and the initial thermal decomposition temperatures, nevertheless the crosslink density affects much the glass temperature of the resulting epoxy network; i.e., the higher the crosslink density, the higher the glass temperature.

As the temperature further rises, the remainder decomposes rapidly in 300–500 °C, with the maximum rate at 381 °C for DGEBA/PADT and 380 °C for DGEBA/propanediamine. This stage of the pyrolysis could be ascribed to the random thermal scission of the network chains to produce the volatile gases. At the even high temperature, the decrease of the weight percentage becomes very slow, leaving about 9–13% residual char at 800 °C. Noticeably, at this temperate the char content of DGEBA/PADT is somewhat lower than that of DGBEA/propanediamine, which is due to the reason below. The higher N–H equivalent weight of PADT leads to its increased stoichiometry relative to DGEBA, thus decreasing the aromatic content in the unit weight of the epoxy-amine mixture. The aromatic content is more liable to carbonize at a higher temperature in an inner atmosphere, due in part to its higher carbon/hydrogen ratio. Hence, after the high-temperature pyrolysis, DGEBA/propanediamine leaves the increased char content compared to DGEBA/PADT. Furthermore, since residual char content can serves as an important index for evaluating flame retardancy of epoxy resins, our result also implicates that to improve the flame retardancy of cured epoxy resins, tailoring basic element compositions and increasing aromatic contents in cured resins are much more effective than increasing the crosslink density alone.

4. Conclusions

PADT has been successfully prepared and systematically characterized, which turned out to able to effectively cure DGEBA (i.e., the high reactivity) with the overall reaction heat of 107.9 kJ/mol epoxide. The isothermal reaction was found autocatalytic in nature. The extended autocatalytic Kamal model coupled with the diffu-

sion term could well simulate the reaction rate over the entire conversion range, and the calculated non-autocatalytic and autocatalytic reaction activation energies were 56.28 ± 2.56 kJ/mol and 50.50 ± 4.30 kJ/mol, respectively. The model-free isoconversional analysis of the reaction effective energy, E_α, revealed that the reaction-controlled kinetics was predominant at the early stage ($\alpha < 0.33$) as reflected by the relatively constant E_α value of ~50 kJ/mol, whereas the diffusion-controlled kinetics occurred in the deep-conversion regime ($\alpha > 0.8$) as indicated by the sharp decrease in E_α. Moreover, the dynamic mechanical analysis showed that the DGEBA/PADT network had the very high elastic modules at the low temperature and its rigidity was fully acceptable for <100 °C, which, certainly, can satisfactorily meet the room-temperature application purposes. The analysis also indicated that the network exhibits three characteristic transitions from the low to high temperature range: (1) the β transition arising from the localized motion of hydroxypropylether segments, (2) the α' transition attributed to the tertiary N^t functionalities inherited from the PADT molecules, and (3) the glass transition due to the cooperative motion of the whole network chains. More importantly, the DGEBA/PADT network was justified to have the much higher crosslink density than the controlled DGEBA/propanediamine network. Furthermore, the TG analysis showed that PADT could impart the cured epoxy resin with the sufficient good thermal stability, with no obvious thermal decomposition observed up to ~300 °C. To conclude, PADT shows a great promise as a brand new aliphatic-amine curing agent for epoxy resins with the extended stoichiometry, high reactivity, extraordinarily high functionalities, improved thermomechanical properties, good thermal stability, and in particular much increased crosslink density of its cured epoxy resin.

Acknowledgments

This work is supported by the Program for Changjiang Scholars and Innovative Research Team in University, China (PCSIRT) and the Major Research Project of Zhejiang Province, China (Grant no. 2006C11192). Special thanks are owed to the reviewers for critically evaluating this submission and offering the constructive suggestions.

References

[1] C.A. May, Epoxy Resins Chemistry and Technology, second ed., Marcel Dekker, Inc, 1988.
[2] E.M. Petrie, Epoxy Adhesive Formulations, McGraw-Hill Publishing, 2006.
[3] H.Q. Pham, M.J. Marks, Encyclopedia of Polymer Science and Technology, Wiley & Sons Inc, 2004.
[4] K. Mitra, Assessing optimal growth of desired species in epoxy polymerization under uncertainty, Chem. Eng. J. 162 (2010) 322–330.
[5] T.-H. Liou, Kinetics study of thermal decomposition of electronic packaging material, Chem. Eng. J. 98 (2004) 39–51.
[6] F.X. Perrin, T.M.H. Nguyen, J.L. Vernet, Chemico-diffusion kinetics and TTT cure diagrams of DGEBA-DGEBF/amine resins cured with phenol catalysts, Eur. Polym. J. 43 (2007) 5107–5120.
[7] Y. Li, F. Xiao, C.P. Wong, Novel, environmentally friendly crosslinking system of an epoxy using an amino acid: tryptophan-cured diglycidyl ether of bisphenol A epoxy, J. Polym. Sci. A: Polym. Chem. 45 (2007) 181–190.
[8] Y. Li, F. Xiao, K.-S. Moon, C.P. Wong, Novel curing agent for lead-free electronics: amino acid, J. Polym. Sci. A: Polym. Chem. 44 (2006) 1020–1027.
[9] J. Wan, B.-G. Li, H. Fan, Z.-Y. Bu, C.-J. Xu, Nonisothermal reaction kinetics of DGEBA with four-armed starlike polyamine with benzene core (MXBDP) as novel curing agent, Thermochim. Acta 510 (2010) 46–52.
[10] J. Wan, B.-G. Li, H. Fan, Z.-Y. Bu, C.-J. Xu, Nonisothermal reaction, thermal stability and dynamic mechanical properties of epoxy system with novel nonlinear multifunctional polyamine hardener, Thermochim. Acta 511 (2010) 51–58.
[11] J. Wan, H. Fan, B.-G. Li, C.-J. Xu, Z.-Y. Bu, Synthesis and nonisothermal reaction of a novel acrylonitrile-capped poly(propyleneimine) dendrimer with epoxy resin, J. Therm. Anal. Calorim. 103 (2011) 685–692.
[12] J. Wan, Z.-Y. Bu, C.-J. Xu, B.-G. Li, H. Fan, Learning about novel amine-adduct curing agents for epoxy resins: butylglycidylether-modified poly(propyleneimine) dendrimers, Thermochim. Acta, doi:10.1016/j.tca.2011.02.038.
[13] H. Cai, P. Li, G. Sui, Y. Yu, G. Li, X. Yang, S. Ryu, Curing kinetics study of epoxy resin/flexible amine toughness systems by dynamic and isothermal DSC, Thermochim. Acta 473 (2008) 101–105.
[14] M.M.d.B.-v.d.B. Ellen, E.W. Meijer, Poly(propylene imine) dendrimers: large-scale synthesis by hetereogeneously catalyzed hydrogenations, Angew. Chem. Int. Ed. Engl. 32 (1993) 1308–1311.
[15] C. Wörner, R. Mülhaupt, Polynitrile- and polyamine-functional poly(trimethylene imine) dendrimers, Angew. Chem. Int. Ed. Engl. 32 (1993) 1306–1308.
[16] B.D. Mather, K. Viswanathan, K.M. Miller, T.E. Long, Michael addition reactions in macromolecular design for emerging technologies, Prog. Polym. Sci. 31 (2006) 487–531.
[17] J.M. Barton, The application of differential scanning calorimetry (DSC) to the study of epoxy resin curing reactions, Adv. Polym. Sci. 72 (1985) 111–154.
[18] M. Ochi, K. Yamashita, M. Shimbo, The mechanism for occurrence of internal stress during curing epoxide resins, J. Appl. Polym. Sci. 43 (1991) 2013–2019.
[19] C.-S. Wu, Influence of post-curing and temperature effects on bulk density, glass transition and stress-strain behaviour of imidazole-cured epoxy network, J. Mater. Sci. 27 (1992) 2952–2959.
[20] J. Mijovic, J.A. Koutsky, Correlation between nodular morphology and fracture properties of cured epoxy resins, Polymer 20 (1979) 1095–1107.
[21] J. Mijovic, L. Tsay, Correlations between dynamic mechanical properties and nodular morphology of cured epoxy resins, Polymer 22 (1981) 902–906.
[22] J. Mijović, J.G. Williams, T. Donnellan, Processing–morphology–property relationships in epoxy resins, J. Appl. Polym. Sci. 30 (1985) 2351–2366.
[23] L. Zhao, X. Hu, A variable reaction order model for prediction of curing kinetics of thermosetting polymers, Polymer 48 (2007) 6125–6133.
[24] R.A. Fava, Differential scanning calorimetry of epoxy resins, Polymer 9 (1968) 137–151.
[25] A. Yousefi, P.G. Lafleur, R. Gauvin, Kinetic studies of thermoset cure reactions: a review, Polym. Compos. 18 (1997) 157–168.
[26] S. Vyazovkin, C.A. Wight, Model-free and model-fitting approaches to kinetic analysis of isothermal and nonisothermal data, Thermochim. Acta 340–341 (1999) 53–68.
[27] S. Vyazovkin, Model-free kinetics staying free of multiplying entities without necessity, J. Therm. Anal. Calorim. 83 (2006) 45–51.
[28] A. Khawam, D.R. Flanagan, Complementary use of model-free and modelistic methods in the analysis of solid-state kinetics, J. Phys. Chem. B 109 (2005) 10073–10080.
[29] A. Khawam, D.R. Flanagan, Role of isoconversional methods in varying activation energies of solid-state kinetics: II. Nonisothermal kinetic studies, Thermochim. Acta 436 (2005) 101–112.
[30] H.J. Borchardt, F. Daniels, The application of differential thermal analysis to the study of reaction kinetics, J. Am. Chem. Soc. 79 (1957) 41–46.
[31] S. Sourour, M.R. Kamal, Differential scanning calorimetry of epoxy cure: isothermal cure kinetics, Thermochim. Acta 14 (1976) 41–59.
[32] R.K. Musa, Thermoset characterization for moldability analysis, Polym. Eng. Sci. 14 (1974) 231–239.
[33] M.R. Kamal, S. Sourour, Kinetics and thermal characterization of thermoset cure, Polym. Eng. Sci. 13 (1973) 59–64.
[34] S. Vyazovkin, N. Sbirrazzuoli, Isoconversional kinetic analysis of thermally stimulated processes in polymers, Macromol. Rapid Commun. 27 (2006) 1515–1532.
[35] H.L. Friedman, Kinetics of thermal degradation of char-forming plastics from thermogravimetry. Application to a phenolic plastic, J. Polym. Sci. C 6 (1964) 183–195.
[36] S. Vyazovkin, Reply to "What is meant by the term 'variable activation energy' when applied in the kinetics analyses of solid state decompositions (crystolysis reactions)?", Thermochim. Acta 397 (2003) 269–271.
[37] J.H. Flynn, L.A. Wall, General treatment of the thermogravimetry of polymers, J. Res. Natl. Bur. Stand. A: Phys. Chem. 70A (1966) 487–523.
[38] T. Ozawa, A new method of analyzing thermogravimetric data, Bull. Chem. Soc. Jpn. 38 (1965) 1881–1886.
[39] S. Vyazovkin, Modification of the integral isoconversional method to account for variation in the activation energy, J. Comput. Chem. 22 (2001) 178–183.
[40] S. Vyazovkin, Evaluation of activation energy of thermally stimulated solid-state reactions under arbitrary variation of temperature, J. Comput. Chem. 18 (1997) 393–402.
[41] S. Vyazovkin, D. Dollimore, Linear and nonlinear procedures in isoconversional computations of the activation energy of nonisothermal reactions in solids, J. Chem. Inf. Comput. Sci. 36 (1996) 42–45.
[42] S. Vyazovkin, N. Sbirrazzuoli, Kinetic analysis of isothermal cures performed below the limiting glass transition temperature, Macromol. Rapid Commun. 21 (2000) 85–90.
[43] S. Vyazovkin, A unified approach to kinetic processing of nonisothermal data, Int. J. Chem. Kinet. 28 (1996) 95–101.
[44] S. Vyazovkin, N. Sbirrazzuoli, Isoconversional method to explore the mechanism and kinetics of multi-step epoxy cures, Macromol. Rapid Commun. 20 (1999) 387–389.
[45] N. Sbirrazzuoli, S. Vyazovkin, Learning about epoxy cure mechanisms from isoconversional analysis of DSC data, Thermochim. Acta 388 (2002) 289–298.
[46] S. Vyazovkin, A. Mititelu, N. Sbirrazzuoli, Kinetics of epoxy–amine curing accompanied by the formation of liquid crystalline structure, Macromol. Rapid Commun. 24 (2003) 1060–1065.
[47] N. Sbirrazzuoli, S. Vyazovkin, A. Mititelu, C. Sladic, L. Vincent, A study of epoxy-amine cure kinetics by combining isoconversional analysis with temperature

modulated DSC and dynamic rheometry, Macromol. Chem. Phys. 204 (2003) 1815–1821.
[48] N. Sbirrazzuoli, A. Mititelu-Mija, L. Vincent, C. Alzina, Isoconversional kinetic analysis of stoichiometric and off-stoichiometric epoxy-amine cures, Thermochim. Acta 447 (2006) 167–177.
[49] Z.-Q. Cai, J. Sun, D. Wang, Q. Zhou, Studies on curing kinetics of a novel combined liquid crystalline epoxy containing tetramethylbiphenyl and aromatic ester-type mesogenic group with diaminodiphenylsulfone, J. Polym. Sci. A: Polym. Chem. 45 (2007) 3922–3928.
[50] A. Kandelbauer, G. Wuzella, A. Mahendran, I. Taudes, P. Widsten, Model-free kinetic analysis of melamine-formaldehyde resin cure, Chem. Eng. J. 152 (2009) 556–565.
[51] J. Wang, M.-P.G. Laborie, M.P. Wolcott, Comparison of model-free kinetic methods for modeling the cure kinetics of commercial phenol-formaldehyde resins, Thermochim. Acta 439 (2005) 68–73.
[52] J. Wang, M.-P.G. Laborie, M.P. Wolcott, Correlation of mechanical and chemical cure development for phenol-formaldehyde resin bonded wood joints, Thermochim. Acta 513 (2011) 20–25.
[53] G. Rivero, V. Pettarin, A. Vázquez, L.B. Manfredi, Curing kinetics of a furan resin and its nanocomposites, Thermochim. Acta 516 (2011) 79–87.
[54] C.C. Riccardi, R.J.J. Williams, Statistical structural model for the build-up of epoxy-amine networks with simultaneous etherification, Polymer 27 (1986) 913–920.
[55] C.C. Riccardi, R.J.J. Williams, A kinetic scheme for an amine-epoxy reaction with simultaneous etherification, J. Appl. Polym. Sci. 32 (1986) 3445–3456.
[56] B.A. Rozenberg, Kinetics, thermodynamics and mechanism of reactions of epoxy oligomers with amines, Adv. Polym. Sci. 75 (1986) 113–165.
[57] J.K. Gillham, J.A.B.A. Noshay, Isothermal transitions of a thermosetting system, J. Appl. Polym. Sci. 18 (1974) 951–961.
[58] S. Montserrat, Vitrification and further structural relaxation in the isothermal curing of an epoxy resin, J. Appl. Polym. Sci. 44 (1992) 545–554.
[59] G. Van Assche, A. Van Hemelrijck, H. Rahier, B. Van Mele, Modulated differential scanning calorimetry: non-isothermal cure, vitrification, and devitrification of thermosetting systems, Thermochim. Acta 286 (1996) 209–224.
[60] S. Montserrat, F.R.P. Colomer, Vitrification, devitrification, and dielectric relaxations during the non-isothermal curing of diepoxy-cycloaliphatic diamine, J. Appl. Polym. Sci. 102 (2006) 558–563.
[61] I. Fraga, J. Hutchinson, S. Montserrat, Vitrification and devitrification during the non-isothermal cure of a thermoset, J. Therm. Anal. Calorim. 99 (2010) 925–929.
[62] M.R. Keenan, Autocatalytic cure kinetics from DSC measurements: zero initial cure rate, J. Appl. Polym. Sci. 33 (1987) 1725–1734.
[63] L. Barral, J. Cano, A.J. López, J. López, P. Nogueira, C. Ramírez, Isothermal cure kinetics of a diglycidyl ether of bisphenol A/1, 3-bisaminomethylcyclohexane (DGEBA/1,3-BAC) epoxy resin system, J. Appl. Polym. Sci. 56 (1995) 1029–1037.
[64] I.T. Smith, The mechanism of the crosslinking of epoxide resins by amines, Polymer 2 (1961) 95–108.
[65] S. Vyazovkin, N. Sbirrazzuoli, Kinetic methods to study isothermal and nonisothermal epoxy-anhydride cure, Macromol. Chem. Phys. 200 (1999) 2294–2303.
[66] G.V. Assche, S. Swier, B.V. Mele, Modeling and experimental verification of the kinetics of reacting polymer systems, Thermochim. Acta 388 (2002) 327–341.
[67] L. Xu, J.H. Fu, J.R. Schlup, In situ near-infrared spectroscopic investigation of epoxy resin-aromatic amine cure mechanisms, J. Am. Chem. Soc. 116 (1994) 2821–2826.
[68] B. Jankovic, The kinetic analysis of isothermal curing reaction of an unsaturated polyester resin: estimation of the density distribution function of the apparent activation energy, Chem. Eng. J. 162 (2010) 331–340.
[69] K.C. Cole, J.J. Hechler, D. Noel, A new approach to modeling the cure kinetics of epoxy/amine thermosetting resins. 2. Application to a typical system based on bis[4-(diglycidylamino)phenyl]methane and bis(4-aminophenyl) sulfone, Macromolecules 24 (1991) 3098–3110.
[70] A.I. Burshtein, Molecular-kinetic aspects of the phemical physics of the condensed state, Russ. Chem. Rev. 47 (1978) 212–234.
[71] M.V. Alonso, M. Oliet, J. García, F. Rodríguez, J. Echeverría, Gelation and isoconversional kinetic analysis of lignin–phenol–formaldehyde resol resins cure, Chem. Eng. J. 122 (2006) 159–166.
[72] X. Wang, J.K. Gillham, Competitive primary amine/epoxy and secondary amine/epoxy reactions: effect on the isothermal time-to-vitrify, J. Appl. Polym. Sci. 43 (1991) 2267–2277.
[73] G. Odian, Principles of Polymerization, fourth ed., John Wiley & Sons, Inc, 2004.
[74] S. Vyazovkin, N. Sbirrazzuoli, Mechanism and kinetics of epoxy-amine cure studied by differential scanning calorimetry, Macromolecules 29 (1996) 1867–1873.
[75] H. Stutz, J. Mertes, Influence of the structure on thermoset cure kinetics, J. Polym. Sci. A: Polym. Chem. 31 (1993) 2031–2037.
[76] H. Stutz, J. Mertes, K. Neubecker, Kinetics of thermoset cure and polymerization in the glass transition region, J. Polym. Sci. A: Polym. Chem. 31 (1993) 1879–1886.
[77] H.S. Chu, J.C. Seferis, Dynamic mechanical experiments for probing process–structure–property relations in amine-cured epoxies, Polym. Compos. 5 (1984) 124–140.
[78] S. Cukierman, J.-L. Halary, L. Monnerie, Dynamic mechanical response of model epoxy networks in the glassy state, Polym. Eng. Sci. 31 (1991) 1476–1482.
[79] F.G. Garcia, B.G. Soares, V.J.R.R. Pita, R. Sánchez, J. Rieumont, Mechanical properties of epoxy networks based on DGEBA and aliphatic amines, J. Appl. Polym. Sci. 106 (2007) 2047–2055.
[80] T. Kamon, H. Furukawa, Curing mechanisms and mechanical properties of cured epoxy resins, Adv. Polym. Sci. 80 (1986) 173–202.
[81] O. Delatycki, J.C. Shaw, J.G. Williams, Viscoelastic properties of epoxy-diamine networks, J. Polym. Sci. B: Polym. Phys. 7 (1969) 753–762.
[82] J.A. Schroeder, P.A. Madsen, R.T. Foister, Structure/property relationships for a series of crosslinked aromatic/aliphatic epoxy mixtures, Polymer 28 (1987) 929–940.
[83] F. Fernandez-Nograro, A. Valea, R. Llano-Ponte, I. Mondragon, Dynamic and mechanical properties of DGEBA/poly(propylene oxide) amine based epoxy resins as a function of stoichiometry, Eur. Polym. J. 32 (1996) 257–266.
[84] J.S. Nakka, K.M.B. Jansen, L.J. Ernst, W.F. Jager, Effect of the epoxy resin chemistry on the viscoelasticity of its cured product, J. Appl. Polym. Sci. 108 (2008) 1414–1420.
[85] A. Shabeer, A. Garg, S. Sundararaman, K. Chandrashekhara, V. Flanigan, S. Kapila, Dynamic mechanical characterization of a soy based epoxy resin system, J. Appl. Polym. Sci. 98 (2005) 1772–1780.
[86] A. Gerbase, C. Petzhold, A. Costa, Dynamic mechanical and thermal behavior of epoxy resins based on soybean oil, J. Am. Oil Chem. Soc. 79 (2002) 797–802.
[87] T. Murayama, J.P. Bell, Relation between the network structure and dynamic mechanical properties of a typical amine-cured epoxy polymer, J. Polym. Sci. B: Polym. Phys. 8 (1970) 437–445.
[88] J.F. Gerard, J. Galy, J.P. Pascault, S. Cukierman, J.L. Halary, Viscoelastic response of model epoxy networks in the glass transition region, Polym. Eng. Sci. 31 (1991) 615–621.